Journal of Power Sources 226 (2013) 82–86

Contents lists available at SciVerse ScienceDirect

Journal of Power Sources

journal homepage: www.elsevier.com/locate/jpowsour

Short communication

Electrospun polyimide nanofiber-based nonwoven separators for lithium-ion batteries

Yue-E Miao [a], Guan-Nan Zhu [b], Haoqing Hou [c], Yong-Yao Xia [b,*], Tianxi Liu [a,*]

[a] State Key Laboratory of Molecular Engineering of Polymers, Department of Macromolecular Science, Fudan University, Shanghai 200433, PR China
[b] Department of Chemistry and Shanghai Key Laboratory of Molecular Catalysis and Innovative Materials, Institute of New Energy, Fudan University, Shanghai 200433, PR China
[c] Department of Chemistry and Chemical Engineering, Jiangxi Normal University, Nanchang 330022, PR China

HIGHLIGHTS

- Polyimide (PI) nanofiber-based nonwovens have been fabricated via electrospinning for separators of LIBs.
- Electrospun PI nanofiber nonwovens show superior thermal stability than that of the commercial Celgard membrane.
- Compared to the Celgard membrane, PI nanofiber nonwovens exhibit better wettability toward electrolyte.
- The electrospun PI nanofiber nonwoven separators present high-performance battery properties.

GRAPHICAL ABSTRACT

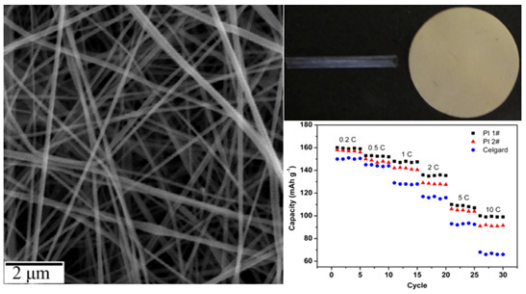

ARTICLE INFO

Article history:
Received 8 September 2012
Received in revised form
10 October 2012
Accepted 12 October 2012
Available online 22 October 2012

Keywords:
Polyimide
Electrospinning
Nonwoven separator
Lithium-ion battery

ABSTRACT

Polyimide (PI) nanofiber-based nonwovens have been fabricated via electrospinning for the separators of lithium-ion batteries (LIBs). Differential scanning calorimetry (DSC), thermogravimetric analysis (TGA) and hot oven tests show that the PI nanofiber-based nonwovens are thermally stable at a high temperature of 500 °C while the commercial Celgard membrane exhibits great shrinkage at 150 °C and even goes melting over 167 °C, indicating a superior thermal stability of PI nanofiber-based nonwovens than that of the Celgard membrane. Moreover, the PI nanofiber-based nonwovens exhibit better wettability for the polar electrolyte compared to the Celgard membrane. The PI nanofiber-based nonwoven separators are also evaluated to have higher capacity, lower resistance and higher rate capability compared to the Celgard membrane separator, which proves that they are ideal candidates for separators of high-performance rechargeable LIBs.

1. Introduction

High-performance rechargeable lithium-ion batteries (LIBs) with long cycle life, high energy and power densities have recently received much attention due to the rapidly growing high energy demands [1,2]. In the LIB system, the separator plays a vital role in preventing electronic contact between electrodes and retaining liquid electrolyte in cells [3–5]. Currently, conventional polyolefin microporous membranes (Celgard) are usually used as separators for most LIBs due to their quite suitable chemical stability, thickness, and mechanical strength. However, several intrinsic factors such as low porosity (about 40%), poor thermal stability and large difference of polarity between the highly polar liquid electrolyte and the nonpolar polyolefin separator lead to high cell resistance,

* Corresponding authors. Tel.: +86 21 55664197; fax: +86 21 65640293.
E-mail addresses: yyxia@fudan.edu.cn (Y.-Y. Xia), txliu@fudan.edu.cn (T.X. Liu).

0378-7753/$ – see front matter © 2012 Elsevier B.V. All rights reserved.
http://dx.doi.org/10.1016/j.jpowsour.2012.10.027

low rate capability and even internal short circuits of LIBs, which severely restricts the electrochemical performance of the LIBs [6–9]. Therefore, the development of new separators having high porosity and thermal stability, good wettability toward liquid electrolyte is considered to be of significant importance for fabricating high-performance rechargeable LIBs.

Given the low cost and ease in the construction of microstructures (e.g., pore size and porosity), nonwoven separators are especially attractive and promising to replace the conventional microporous polyolefin membranes. Some novel methods have been applied to fabricate fibrous nonwovens as the separators of LIBs, such as the paper-making method [10], solution extrusion method via a spinning jet [11], and the melt blowing method [12]. Electrospinning is a promising and straightforward technique that produces continuous fibers with diameters in the range of nanometers to a few microns [13,14]. Electrospun fiber membranes thus obtained possess smaller pore size, higher porosity and air permeability compared to the conventional nonwovens, making them excellent candidates for separators in rechargeable LIBs. Electrospun polyacrylonitrile and poly(vinylidene fluoride) nanofiber-based nonwovens have already been developed and evaluated in LIBs and exhibited outstanding battery performances, such as large capacity, high-rate capability and long cycle life [15–17].

Polyimide (PI), as one kind of high-performance engineering polymers, has been widely used in many advanced technology fields due to their excellent thermal stability, outstanding mechanical properties, low dielectric constants and inertness to solvent and radiation resistance. Therefore, electrospun PI nanofiber membranes with diverse molecular structures, controllable fiber diameters and membrane thicknesses have been intensively investigated to obtain high-performance and multifunctional composite fiber membranes [18–20]. In our previous studies [19,20], highly aligned polyimide nanofiber membranes were prepared by electrospinning equipped with a high speed rotating collector, which showed excellent mechanical and thermal properties. PI is thermally stable at temperatures over 500 °C, which can effectively avoid the short circuits caused by the shrinkage of the conventional separators at high temperature of 150 °C. Moreover, polar solvents such as ethylene carbonate (EC) and ethyl methyl carbonate (EMC) can be strongly coordinated within the polymer chains due to the electron donor and acceptor groups of PI, which will largely enhance the retain ability for electrolyte of PI-based battery separators. Therefore, polyimide nanofiber-based nonwovens with different thicknesses are fabricated via electrospinning for the separators of LIBs in this research. Superior thermal and electrochemical properties of the PI nanofiber-based nonwovens indicate that they are ideal separator candidates for LIBs to achieve high battery performance, such as large capacity, high-rate capability and long cycle life.

2. Experimental

2.1. Materials

Pyromellitic dianhydride (PMDA), 4,4′-oxydianiline (ODA), and N,N-dimethylacetamide (DMAc) were commercially obtained from China Medicine Co. The Celgard membrane (Celgard, China) with a thickness of about 30 μm was used as the separator of LIBs for a comparative study. All other reactants were of analytical purity and used as received.

2.2. Preparation of electrospun PI nanofiber membranes

The precursor of polyimide, poly(amic acid) (PAA) was synthesized via the polycondensation of PMDA and ODA with an equivalent molar ratio in DMAc (N,N-dimethylacetamide) at −3 °C, thus obtaining the pristine PAA solution with the solid content of 15%. Electrospinning was carried out using a syringe with a spinneret having a diameter of 0.5 mm at an applied voltage of 18–25 kV. The PAA solution was fed at a speed of 0.25 mL h^{-1} with a distance of 20 cm between tip of the needle and the collector. By controlling the deposition time of the electrospinning process, PAA nanofiber membranes with different thicknesses (40 μm and 100 μm for PI no.1 and PI no.2 nanofiber-based nonwovens, respectively) can be easily obtained. All the electrospun nanofiber membranes were overnight dried at 60 °C to remove the residual solvent and then thermally imidized to obtain PI nanofibers using the following program: heating up at a rate of 3 °C min^{-1} to 100, 200 and 300 °C, followed by an annealing at each temperature stage for 30 min.

2.3. Characterization

Fourier transform infrared (FTIR) spectra were obtained in the range of 4000–400 cm^{-1} with a 4 cm^{-1} spectral resolution on a Nicolet Nexus 470 spectrometer. The morphology and fiber diameters of the samples were investigated using scanning electron microscope (SEM, Tescan) at an acceleration voltage of 20 kV. The thermal property of the samples was measured by differential scanning calorimetry (DSC) in the temperature range of 50–240 °C at a heating rate of 10 °C min^{-1} using a TA DSC 2920. Thermogravimetric analysis (Pyris 1 TGA) was performed under air flow from 100 to 800 °C at a heating rate of 20 °C min^{-1}. Static contact angle measurements were carried out using a commercial drop shape analysis system (Data Physics SCA20, Germany). Air's Gurley values were obtained using the commercial air permeability instrument (Gurley 4110, America).

In order to investigate the rate capability for the cells with various separators, a coin-type cell (CR2016) was used in half-cell configuration assembled in a configuration of $Li_4Ti_5O_{12}$/separator/lithium metal. $Li_4Ti_5O_{12}$ was prepared in a conventional solid-state process as described previously [21]. During the rate-performance tests, the cell was first charged up to 3.0 V at the 0.2 C (32 mA g^{-1}) rate, and then discharged to 1.0 V at different current rates of 0.2, 0.5, 1, 2, 5 and 10 C.

The ionic conductivities of different separators including the Celgard membrane, electrospun PI no.1 and PI no.2 nanofiber-based nonwovens were measured by electrochemical impedance spectroscopy (EIS) using a Solartron Instrument Model 1287 electrochemical interface and 1255B frequency response analyzer controlled by a computer. During the measurements, the liquid electrolyte-soaked separators were sandwiched between two symmetrical stainless-steel plate electrodes and sealed. The impedance measurements were performed at an amplitude of 10 mV over a frequency range of 10^5 to 1 Hz.

3. Results and discussion

3.1. Physical properties

Imidization of PAA has been confirmed by FTIR as shown in Fig. 1. The absorption peaks attributed to N–H and O–H bonds did not appear in the range from 3000 to 4000 cm^{-1} in the FTIR spectrum of the PI nanofiber-based nonwoven, which indicates that the PAA nonwoven has been effectively converted into the corresponding PI nonwoven by thermal imidization.

The morphology and fiber diameters of PI nanofibers were investigated by SEM, as shown in Fig. 2a and b. The diameter of the as-prepared nanofibers is uniform with an average size of around 200 nm. At a higher magnification, it can be seen that the surface of the electrospun nanofibers is smooth and almost free of defects such as beads, which is of vital importance to provide nonwovens

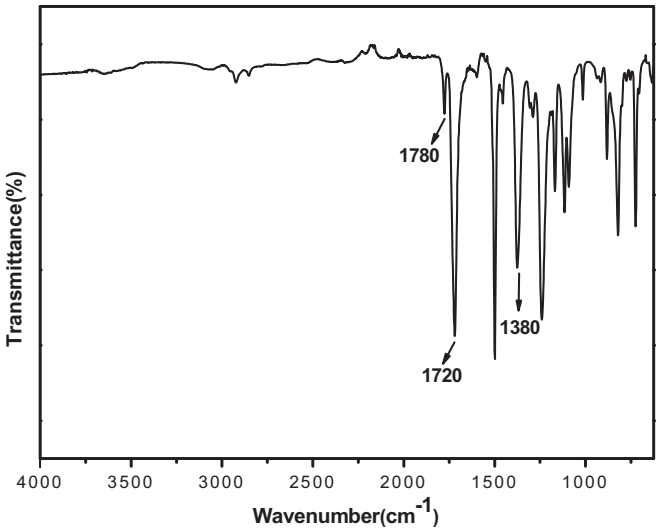

Fig. 1. FTIR spectrum of PI no. 1 nanofiber nonwoven.

with good mechanical strength and prevent the internal short circuit of the cells during the charge–discharge tests. Since the minimum diameter of the conventional Celgard membrane is about 1 μm [7] while PI nanofibers obtained by electrospinning possess smaller diameter, higher porosity and air permeability, they are excellent candidates for separators of high power lithium ion batteries.

The thermal stability of the separators was first evaluated by DSC (Fig. 3a). The Celgard membrane separator shows an endothermic peak at 167 °C, which is the typical melting temperature of polypropylene. Whereas, no peaks can be observed up to 240 °C for the PI nanofiber-based nonwoven separator, which indicates that the thermal stability of PI is much better than that of Celgard. TGA was also carried out to explore the thermal property of the separators (Fig. 3b). It can be seen that the onset temperature of degradation (T_{onset}) of PI is over 500 °C, which is twice that of Celgard, further demonstrating the superior thermal stability of PI. Fig. 4 shows the digital pictures of the Celgard membrane and PI nanofiber-based nonwovens before (Fig. 4a–c) and after (Fig. 4d–f) the hot oven tests at 150 °C for 1 h. It can be seen that the Celgard membrane exhibits great shrinkage with the color change from white to transparent, while for the PI nanofiber-based nonwovens no color change and shrinkage are observed after the hot oven tests.

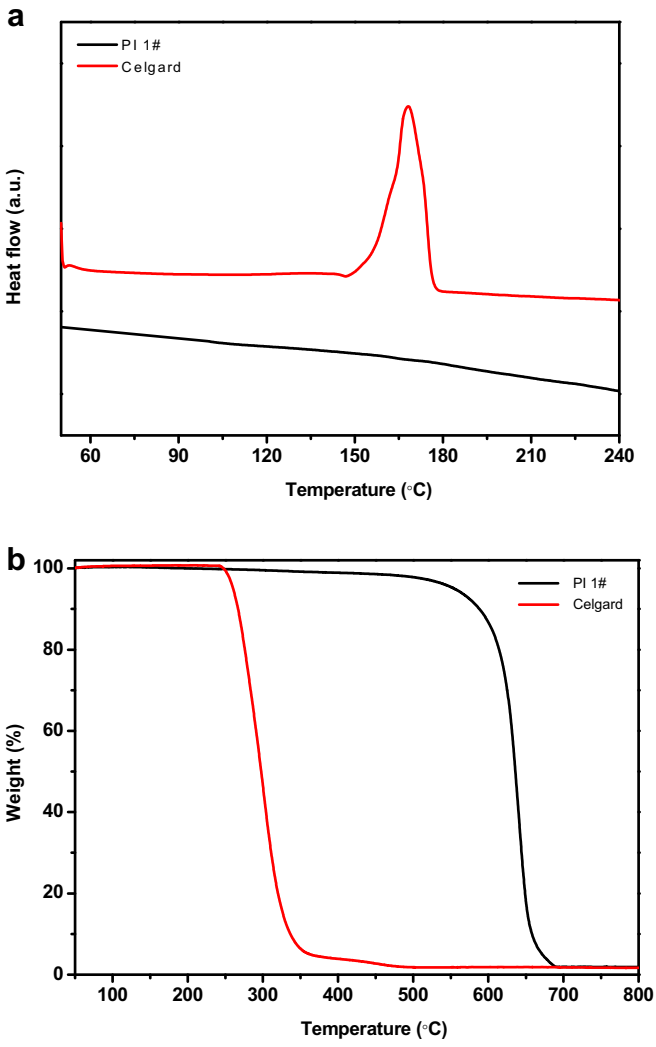

Fig. 3. (a) DSC and (b) TGA curves of Celgard membrane and PI no. 1 nanofiber nonwoven.

Thus, it can be expected that the thermal stability of the lithium ion batteries will be significantly improved when PI nanofiber-based nonwovens are applied as battery separators.

The wettability of the separators in non-aqueous electrolyte is evaluated by contact angle measurements. The contact angle of the

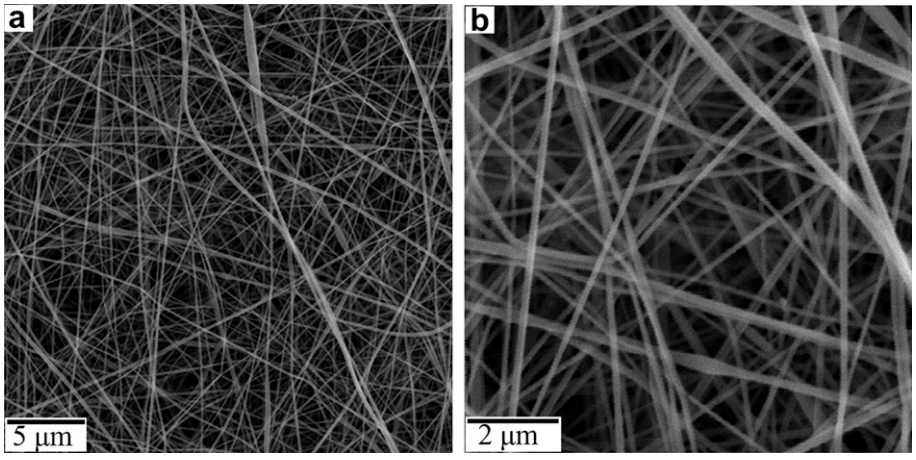

Fig. 2. SEM images at low (a) and high (b) magnifications for PI no. 1 nanofiber nonwoven.

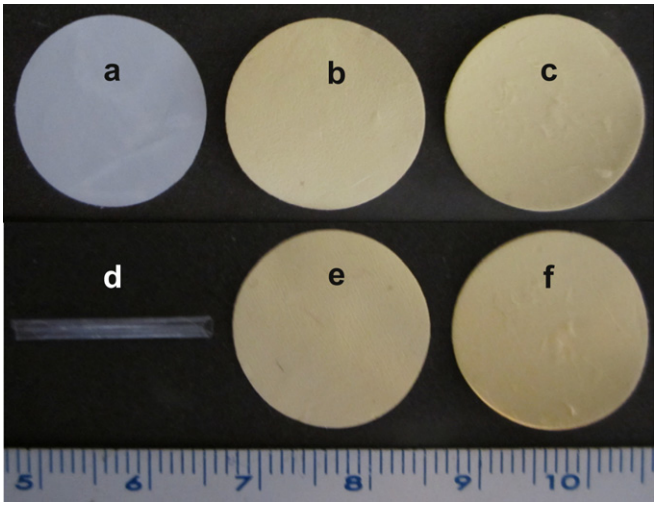

Fig. 4. Digital pictures of (a) Celgard membrane, (b) PI no. 1 and (c) PI no. 2 nanofiber nonwovens before hot oven tests; (d) Celgard membrane, (e) PI no. 1 and (f) PI no. 2 nanofiber nonwovens after hot oven tests.

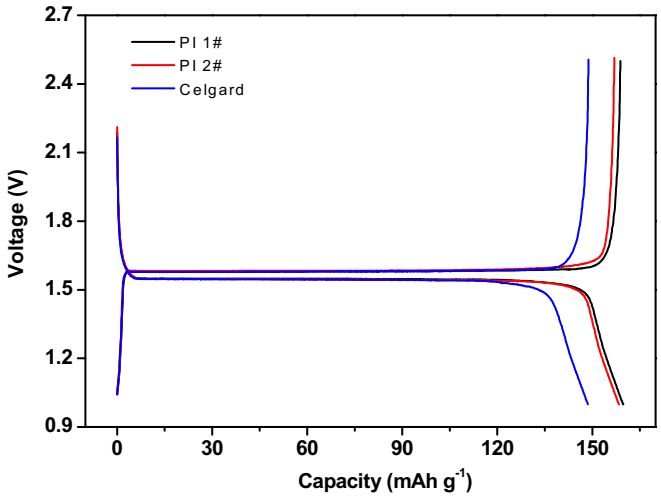

Fig. 6. Initial charge–discharge curves for the cells using Celgard membrane, PI no. 1 and PI no. 2 nanofiber nonwovens as separators, respectively.

PI nanofiber-based nonwovens decreases more rapidly than that of the Celgard membrane during the dynamic process. After the same contact time with the electrolyte, PI nanofiber-based nonwovens show better wettability for the electrolyte compared to the Celgard membrane, as shown in Fig. 5, which can be attributed to the close polarity between the polar PI nanofiber-based nonwoven separators and the highly polar liquid electrolyte. The higher polarity and porosity of the PI nanofiber-based nonwovens guarantee the penetration and high uptake percentage of the electrolyte.

3.2. Electrochemical properties

Fig. 6 shows the initial charge–discharge curves at the 0.2 C rate for the cells using the Celgard membrane and PI nanofiber-based nonwovens as separators. All the curves show stable charge and discharge plateaus with discharge capacities of 150, 158 and 160 mA h g^{-1} for the Celgard membrane, PI no. 1 and PI no. 2 nanofiber-based nonwovens, respectively. Due to the smaller diameter, higher porosity and better wettability for the electrolyte, the capacities of PI nanofiber-based nonwovens are higher than that of the Celgard membrane separator.

The rate capabilities of the separators were investigated by applying various current densities on the cells. The cells were discharged at 0.2 C first, and then the rate was gradually increased to 10 C while maintaining each rate constant for 5 cycles (Fig. 7). Both the PI nanofiber-based nonwoven separators show excellent capacity retention of about 90% while the Celgard membrane decreases rapidly to 80% at 1 C rate. Up to the 5 C rate, the PI nanofiber-based nonwoven separators maintain more than 70% of the initial capacity obtained at the 0.2 C rate. However, the Celgard membrane shows a low retention ratio of only about 56% of the initial value. An even large difference of the capacity retention ratio of the cells is observed at the 10 C rate: the capacity retention ratios of the Celgard membrane, PI no. 1 and PI no. 2 nanofiber-based nonwovens are 45%, 62% and 56%, respectively. These results suggest that PI nanofiber-based nonwoven separators show superior performance than that of the conventional Celgard separator in a wide current range, which are suitable for high-rate applications of LIBs. In addition, the rate capability of PI no. 1 nanofiber-based nonwoven surpasses that of PI no. 2 nanofiber-based nonwoven all along, which may be attributed to the lower resistance of PI no. 1 nanofiber-based nonwoven.

To further clarify the difference in rate capability between the samples, EIS, as a useful tool to investigate diffusion issues, was carried out to identify the relationship between the electrochemical performance and electrode kinetics. Nyquist plots of the cells are shown in Fig. 8. The intermediate-frequency semicircle of the Nyquist plot represents the charge-transfer resistance (R_{ct}) related to lithium ion interfacial transfer. As shown in Fig. 8, the order of R_{ct} values is: PI no. 1 (90 Ω) < PI no. 2 (110 Ω) < Celgard (160 Ω). The different charge-transfer resistance between the Celgard membrane and PI nanofiber-based nonwovens could be attributed to the structure of separators, i.e., porosity, polarity and membrane thickness. The higher porosity and better wettability of PI nanofiber-based nonwovens than those of the Celgard membrane are beneficial for the infiltration of the separators by the liquid electrolyte, which facilitates the migration of lithium ions at the electrode/electrolyte interface and leads to a decrease in the cell resistance. From the R_{ct} values of PI no.1 and PI no.2 nanofiber-based cells, it can be seen that the membrane with smaller thickness has lower resistance. To further explore the differences of the rate performance and EIS impedance between PI no. 1 and PI no. 2 nanofiber-based cells, air's Gurley values of PI no. 1 and PI no. 2

Fig. 5. Digital pictures of static contact angles of (a) Celgard membrane, (b) PI no. 1 and (c) PI no. 2 nanofiber nonwovens.

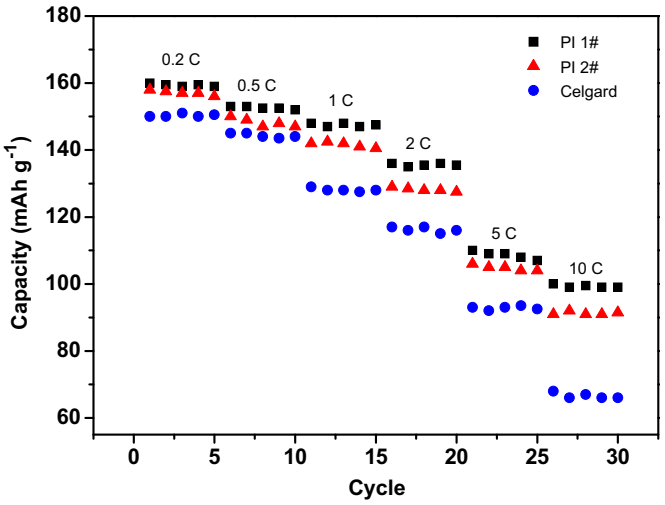

Fig. 7. Rate capability tests for the cells with Celgard membrane, PI no. 1 and PI no. 2 nanofiber nonwovens as separators, respectively.

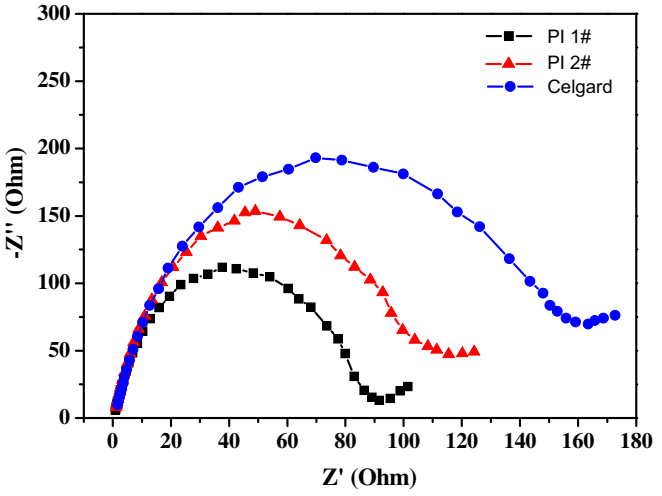

Fig. 8. Nyquist plots for the cells with Celgard membrane, PI no. 1 and PI no. 2 nanofiber nonwovens as separators, respectively.

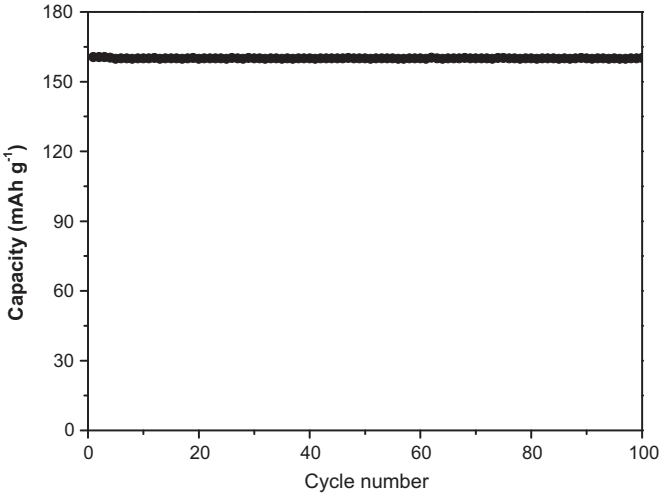

Fig. 9. Cycle performance for the cell with PI no. 1 nanofiber nonwoven separator at 0.2 C rate.

nanofiber-based nonwovens have been carried out. The lower Gurley value (3 s (100 cc)$^{-1}$) of PI no. 1 nanofiber-based nonwoven than that (9 s (100 cc)$^{-1}$) of PI no. 2 nanofiber-based nonwoven is due to its smaller thickness, thus resulting in the lower resistance of PI no. 1 nanofiber-based nonwoven and promoting the penetration of the electrolyte and the migration of lithium ions for better battery performance.

The cycle test of the cell with PI no. 1 was conducted to further investigate the electrochemical stability of PI nanofiber-based nonwoven separators. From Fig. 9, it can be seen that the PI nanofiber-based nonwoven separator shows the capacity retention of almost 100% after 100 cycles at 0.2 C rate, which confirms an excellent efficiency of the nonwoven to conduct lithium ions between electrodes during the cycling process. Therefore, PI nanofiber-based nonwovens are promising candidates for separator of rechargeable LIBs.

4. Conclusions

Polyimide nanofiber-based nonwovens with different thicknesses have been successfully fabricated via electrospinning for the separators of LIBs. The PI nanofiber-based nonwovens are thermally stable at a high temperature of 500 °C while the Celgard membrane exhibits severe shrinkage at 150 °C and even goes melting over 167 °C, indicating the superior thermal stability of the polyimide nanofiber-based nonwoven separators than that of the Celgard membrane separator. Contact angle measurements show that the polar PI nanofiber-based nonwovens have better wettability for the electrolyte compared to the Celgard membrane. The PI nanofiber-based nonwoven separators are also evaluated to have higher capacity, lower resistance and higher rate capability compared to the Celgard membrane separator, indicating that they are ideal candidates for separator of LIBs to achieve high battery performance.

Acknowledgments

The authors are grateful for the financial support from the National Natural Science Foundation of China (51125011).

References

[1] Y.-G. Guo, J.-S. Hu, L.-J. Wan, Adv. Mater. 20 (2008) 2878–2887.
[2] A. Manthiram, A. Vadivel Murugan, A. Sarkar, T. Muraliganth, Energy Environ. Sci. 1 (2008) 621–638.
[3] K. Gao, X. Hu, C. Dai, T. Yi, Mater. Sci. Eng., B 131 (2006) 100–105.
[4] Y. Liang, L. Ji, B. Guo, Z. Lin, Y. Yao, Y. Li, M. Alcoutlabi, Y. Qiu, X. Zhang, J. Power Sources 196 (2011) 436–441.
[5] D. Bansal, B. Meyer, M. Salomon, J. Power Sources 178 (2008) 848–851.
[6] K.M. Abraham, M. Alamgir, D.K. Hoffman, J. Electrochem. Soc. 142 (1995) 683–687.
[7] T.H. Cho, T. Sakai, S. Tanase, K. Kimura, Y. Kondo, T. Tarao, M. Tanaka, Electrochem. Solid-State Lett. 10 (2007) A159–A162.
[8] S.S. Zhang, J. Power Sources 164 (2007) 351–364.
[9] Y.M. Lee, J.-W. Kim, N.-S. Choi, J.A. Lee, W.-H. Seol, J.-K. Park, J. Power Sources 139 (2005) 235–241.
[10] A. Mathur, U.S. Patent 6,517,676, 2003.
[11] S.J. Law, H. Street, G.J. Askew, U.S. Patent 6,358,461, 2002.
[12] Y. Sudou, H. Suzuki, S. Nagami, K. Ikuta, T. Yamamoto, S. Okijima, S. Suzuki, H. Ueshima, U.S. Patent Appl. 20060073389, 2006.
[13] J.B. Fenn, M. Mann, C.K. Meng, S.F. Wong, C.M. Whitehouse, Science 246 (1989) 64–71.
[14] D.-J. Yang, I. Kamienchick, D.Y. Youn, A. Rothschild, I.-D. Kim, Adv. Funct. Mater. 20 (2010) 4258–4264.
[15] T.-H. Cho, M. Tanaka, H. Onishi, Y. Kondo, T. Nakamura, H. Yamazaki, S. Tanase, T. Sakai, J. Power Sources 181 (2008) 155–160.
[16] C. Yang, Z. Jia, Z. Guan, L. Wang, J. Power Sources 189 (2009) 716–720.
[17] N. Wu, Q. Cao, X. Wang, S. Li, X. Li, H. Deng, J. Power Sources 196 (2011) 9751–9756.
[18] L.S. Carnell, E.J. Siochi, N.M. Holloway, R.M. Stephens, C. Rhim, L.E. Niklason, R.L. Clark, Macromolecules 41 (2008) 5345–5349.
[19] D. Chen, T.X. Liu, X.P. Zhou, W.W. Tjiu, H.Q. Hou, J. Phys. Chem. B 113 (2009) 9741–9748.
[20] D. Chen, R.Y. Wang, W.W. Tjiu, T.X. Liu, Compos. Sci. Technol. 71 (2011) 1556–1562.
[21] L. Cheng, X.L. Li, H.J. Liu, H.M. Xiong, P.W. Zhang, Y.Y. Xia, J. Electrochem. Soc. 154 (2007) A692–A697.